| | |
|---|---|
| Title | Safety Evaluation of I-Girder Bridge Repaired by Welding(Mechanics, Strength & Structural Design) |
| Author(s) | Lee, Sang-Hyong; Chang, Kyong-Ho; Kim, You-Chul |
| Citation | Transactions of JWRI. 2003, 32(2), p. 355-362 |
| Version Type | VoR |
| URL | https://doi.org/10.18910/4966 |
| rights | |
| Note | |

# Safety Evaluation of I-Girder Bridge Repaired by Welding

LEE Sang-Hyong*, CHANG Kyong-Ho** and KIM You-Chul***

**Abstract**

*It is often expected that steel structures, which have been damaged by an increase of vehicle load, corrosion, and so on, need repair or strengthening. For repair or strengthening, the evaluation of the safety of damaged structures is usually performed. The estimation of the safety of structures, which are subjected to heating, such as cutting and welding, in procedures of repair or strengthening, is difficult but important. However, the safety evaluation methods of damaged structures following repair or strengthening are not yet well enough established.*

*In this paper, a correction coefficient and the equation of load-carrying-capacity with respect to heat input for the safety evaluation of damaged structures following repair or strengthening were proposed. The validity of this correction coefficient and the equation of load-carrying capacity was confirmed by repair welding experiments and 3-D thermal elastic-plastic FEM analysis of a damaged I-Girder bridge. According to the results, tensile residual stress was generated on account of shrinkage after heating. After the repair work, the residual camber displacement was increased.*

**KEY WORDS :** (Repair welding), (Stress), (Distortion), (FEM)

## 1. Introduction

Steels, which are usually used for structures such as bridges, marine structures, towers, pipes, vessels, and so forth, have characteristics that are apt to promote corrosion quickly and have thin plate structures. It is frequently expected that steel bridges, which have been damaged by an increase of vehicle load, corrosion and so on, need repair or strengthening. There are a number of methods to repair damaged steel structures. For instance, in the case of small size damage, the establishment of a stop-hole, and a re-melting by welding is generally used to prevent the crack progress. In the case of large size damage, replacement after cutting out the damaged part is usually used. These repair or strengthening methods generally are accomplished by cutting, bolting and welding procedures. Among these repair or strengthening methods, the establishment of stop-hole and replacement with bolting have faults like local stress concentrations and an increasing dead load. Other repair or strengthening methods also have some problems with respect to safety at work due to a loss of stiffness.

Among these methods, welding repair method is considered. And the confidence about the safety of the structure during work and after work has to be established. The evaluation method for the load-carrying-capacity in order to evaluate the safety of the structure following the welding repair procedure has to be proposed. Therefore, the stress generated by heating during welding repair procedure is generalized. With a generalized stress pattern, a correction coefficient with respect to heat input under load, such as welding repair work, was decided. In order to confirm the validity of the correction coefficient, repair welding experiments and 3-D thermal elastic-plastic FEM analyses of a damaged I-Girder bridge are carried out.

## 2. Generalized Welding Stress

### 2.1 General

In general, the influence of heating on load-carrying-capacity can be determined through the analysis of the stress pattern generated by heating such as welding. It is known that the average temperature rise($T_{av}$) and initial temperature($\theta_i$) are the parameters governing the stress generated by heating. It has been shown that the average temperature rise($T_{av}$) is :

† Received on December 1st, 2003

* Foreign Guest Researcher
** Assistant Professor, Chung-Ang Univ., Korea
*** Professor

Transactions of JWRI is published by Joining and Welding Research Institute of Osaka University, Ibaraki, Osaka 567-0047, Japan

**Table 1 Welding conditions**

| No. | V(V) | I(A) | $\eta$ | $v$ | $c$ | $\rho$ | $h$ | $B$ | $T_{av}$ |
|---|---|---|---|---|---|---|---|---|---|
| 1 | 30 | 330 | 0.85 | 5 | 0.13 | 7.8 | 8 | 500 | 49.8 |
| 2 | 30 | 265 | 0.85 | 5 | 0.13 | 7.8 | 8 | 500 | 40 |
| 3 | 30 | 200 | 0.85 | 5 | 0.13 | 7.8 | 8 | 500 | 30.2 |
| 4 | 30 | 240 | 0.85 | 5 | 0.13 | 7.8 | 6 | 500 | 48.3 |
| 5 | 30 | 200 | 0.85 | 5 | 0.13 | 7.8 | 6 | 500 | 40.2 |
| 6 | 30 | 150 | 0.85 | 5 | 0.13 | 7.8 | 6 | 500 | 30.2 |

**Table 2 Loading conditions**

| Load | 20 | 40 | 60 |
|---|---|---|---|
| Comp. & Ten. | ○ | ○ | ○ |
| | ○ | ○ | ○ |
| | ○ | ○ | ○ |
| | ○ | ○ | ○ |
| | ○ | ○ | ○ |
| | ○ | ○ | ○ |

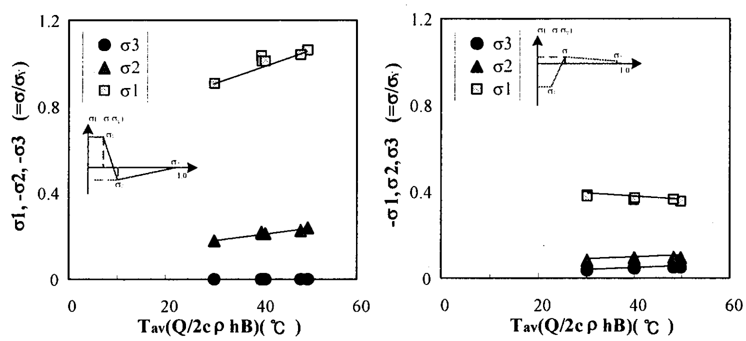


(a) Transient Stress (b) Residual Stress

**Fig. 1 Effect of the average temperature rise on stress generated by welding.**

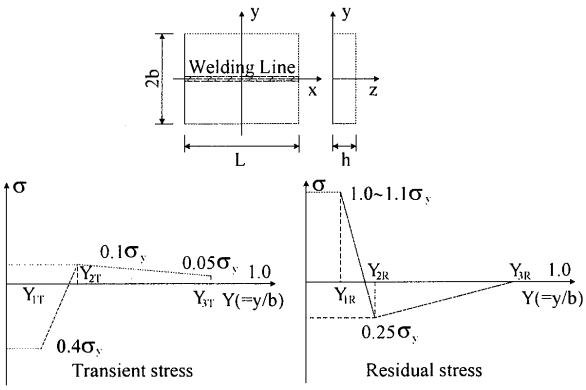


**Fig. 2 Basic shape of distribution of welding stress.**

$$T_{av} = \frac{Q}{2c\rho hB}$$ : the parameter of average temperature rise(℃) (1)

where, $Q = \eta \frac{VI}{v} \times 0.24\ (cal/cm)$,

$c$ = Specific heat($cal/℃ \cdot g$),

$\rho$ = Density($g/cm^3$),

$h$ = Thickness($mm$),

$B$ = Width($mm$),

$V$ = Voltage($V$),

$I$ = Current($A$),

$v$ = Welding speed($mm/\sec$)

The steel materials, which are usually used in the civil engineering, can be characterized by:

$$B \geq 10^{-2} Q/h \quad \text{or} \quad T_{av} \leq 50 \qquad (2)$$

where, $Q$ = Heat input($cal/cm$),

$h$ = Thickness($mm$),

$B$ = Width($mm$)

In order to analyze the stress pattern generated by welding, 3-D thermal elasto-plastic FEM analyses with conditions as in **Table 1** and **Table 2** are carried out.

## 2.2 Distribution of welding residual stress

The relation between stress generated by welding and the average temperature rise is shown in **Fig 1**. From Fig 1, it can be known that the magnitude of stress $\sigma_1, \sigma_2$, and $\sigma_3$ of each diverging point is altered in proportion to the average temperature rise. So, it can be recognized that the stress generated by welding is generally distributed like **Fig 2**

## 2.3 Distribution of welding residual stress under static load

**Figure 3** shows the relation between stress generated by welding under loading and the average temperature rise. From Figure 3, it can be seen that the magnitude of stress $\sigma_1, \sigma_2$, and $\sigma_3$ rises in proportion to the average temperature rise. And also, the applied load has no effect on tensile stress generated by heating such as welding. But, compressive stress has an influence for about half the applied load. Therefore, stress generated by welding under loading is generally distributed as **Fig 4**.

## 2.4 Welding residual stress correction coefficient

There are several methods to evaluate the load-carrying-capacity of structures. For instance, methods, which are based on the allowable stress design theory, LRFD theory, and probability index, are generally used. The method with allowable stress design theory is usually used in steel structures. But, these methods have no regard for heating due to cutting and welding during repair procedures of damaged structures. With the stress correction coefficient with respect to heating, the evaluation of load-carrying-capacity would have been possible during the welding repair work. So, a correction coefficient including the influence of the stress generated by welding, with and without loading, is employed.

**Figure 5** shows the magnitude of stress $\sigma_1$ and $\sigma_2$. Damage such as corrosion is usually found on the lower flange or the lower part of the web of I-Girder bridges. It is known a tensile load is commonly applied on the lower flange of I-Girder bridges. So, safety in repair work can be decided in connection with the transient tensile stress. It can be assumed that the static load has only an effect on the compressive stress generated by welding. Therefore, a stress correction coefficient by welding under loading is employed:

$$K_{HT} = 0.9$$

### 2.5 Equation of load-carrying-capacity with heating

The equation of load-carrying-capacity is expressed as :

$$P' = P \times K_S \times K_r \times K_t \times K_o$$

where, $P = 24 \times \frac{\sigma_a - \sigma_d}{\sigma_{24}}$,

$K$ : Correction Coefficient with respect to each condition,

$\sigma_a$ : Allowable stress,

$\sigma_d$ : Stress of dead load,

$\sigma_{24}$ : Stress of load depend on grade of bridge

The equation of load-carrying-capacity with heating such as welding and cutting accompanied with repair procedure is proposed:

$$P' = P \times K_S \times K_r \times K_t \times K_o \times K_{HT}$$

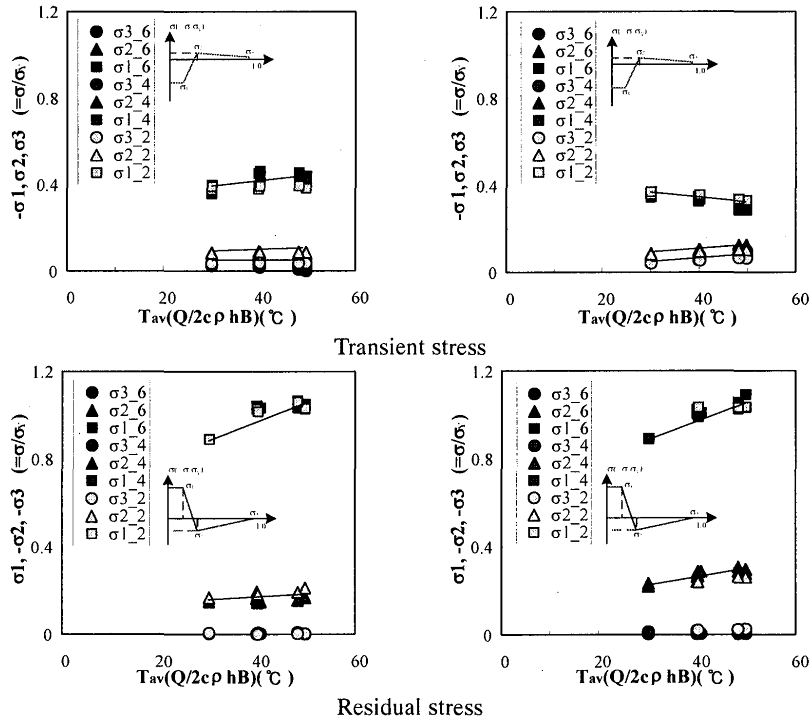


(a) With compressive load (b) With tension load

**Fig. 3 Effect of the average temperature rise on stress generated by welding under loading**

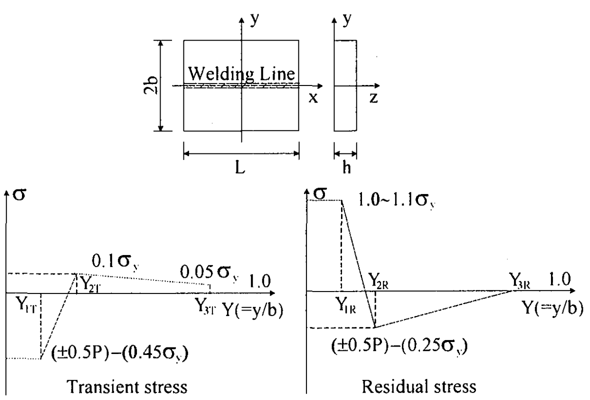


**Fig. 4 Basic shape of distribution of welding stress.**

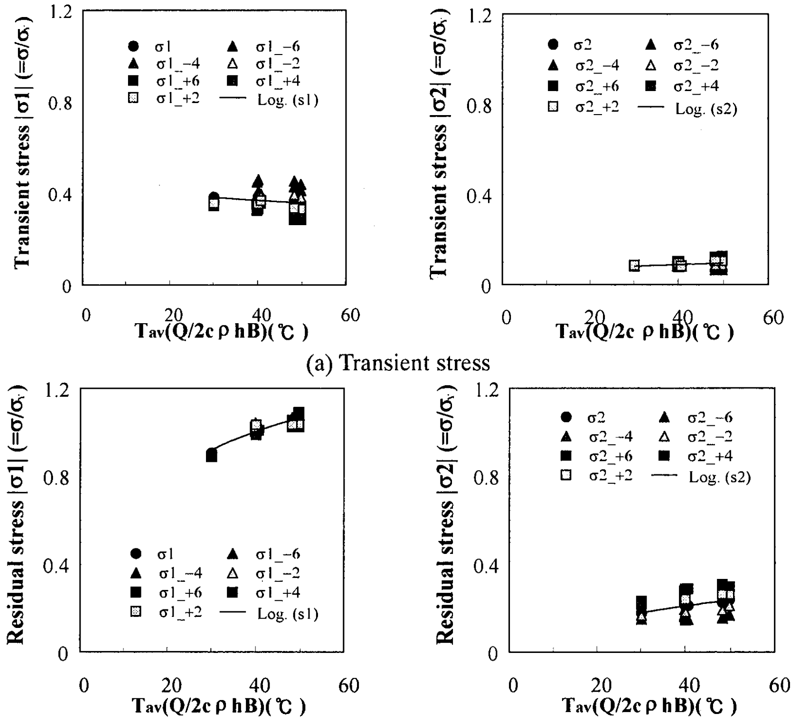
(a) Transient stress
(b) Residual stress

**Fig. 5 Effect of the average temperature rise on residual stress.**

## 3. Experiment and FEM Analysis

In order to confirm the validity of the correction coefficient and the equation of load-carrying-capacity at the repair work, a repair welding experiment and 3-D thermal elastic-plastic FEM analysis of a damaged I-Girder bridge was carried out.

### 3.1 Experiment

*3.1.1 Specification of bridge*

**Figure 6** shows the shape, size and coordinate systems of the experimental object. And the **Table 3** shows the chemical composition and mechanical properties of the steel used for the experimental object.

The 2-span I-girder bridge makes up the upper plate of thickness $16mm$, lower plate of thickness $22mm$ and web of thickness $12mm$. The base metal is SM490B. The strength of the deck plate concrete is $F_{ck} = 300kg/cm^2$.

*3.1.2 Conditions of repair welding*

Figure 6 shows the location of the repair welding experiment. The web of size $750\times180mm$ and lower flange of size $750\times300mm$ are cut out by gas(**Figure 7**). Then, repair is done by welding(**Figure 8**).

**Table 4** shows cutting conditions. Repair welding is performed by FCAW(Flux Cored Arc Welding) under the welding conditions of **Table 5**. The groove angle is 30 degree.

*3.1.3 Loading conditions*

The loading conditions of the repair welding experiment are a weight of $12ton$ of used aggregate and concrete blocks.

*3.1.4 Experimental procedure*

In this paper, a method of repair, strengthening and complement of faults of existing repair methods by welding is proposed. The procedure of proposed repair method is as follows and is shown in **Fig 9**.

(a) Cut out the damaged web section
(b) Cut out the damaged lower flange section
(c) The grinding and making of the groove
(d) Welding of the new web section
(e) Welding of the new lower flange section

*3.1.5 Technical investigation through the welding stress correction coefficient*

A structural analysis was carried out in order to confirm the validity of the welding stress correction coefficient. **Table 6** shows the results of the structural analysis. As a result, the load-carrying-capacity of the experimental object is calculated for the repair work.

The load-carrying-capacity of the experimental object is:

$$P = 18\times\frac{190-38}{1.3\times55} = 38.27ton$$

$$P' = 38.27\times1.2\times1.0\times1.0\times0.95 = 43.6ton$$

And, the load-carrying-capacity incorporating the correction coefficient during welding is:

$$P' = 43.6\times0.9$$
$$= 39.3ton \ \geq 32.4ton$$

**Table 3 Chemical & mechanical properties of bridge.**

| | Chemical composition (%) | | | | | Mechanical properties | | | |
|---|---|---|---|---|---|---|---|---|---|
| SM490B | C | Si | Mn | P | S | Yield Stress (MPa) | Tensile Strength (MPa) | Elongation (%) | Young's modulus (GPa) |
| | 0.18 | 0.55 | 1.5 | 0.04 | 0.04 | 330 | 500 | 17 | 205.3 |

**Table 4 Cutting conditions.**

| Order | Cutting speed $v(mm/\min)$ | | Remarks |
|---|---|---|---|
| 1 | 276 | | Kerf for the Cutting about $2mm$ |
| 2 | 291 | | |
| 3 | 257 | | |
| 4 | 228 | | |
| 5 | | 138 | |
| 6 | | 156 | |

**Table 5 Welding conditions.**

| | Welding speed $v(mm/\sec)$ | | | Current (A) | Voltage (V) | Heat Input $(J/mm)$ |
|---|---|---|---|---|---|---|
| | 1Pass | 2Pass | 3Pass | | | |
| Flange | 2.97 | 2.95 | 2.58 | 240 | 40 | 2880 |
| Web | 2.75 | 2.21 | 2.98 | 240 | 35 | 2770 |

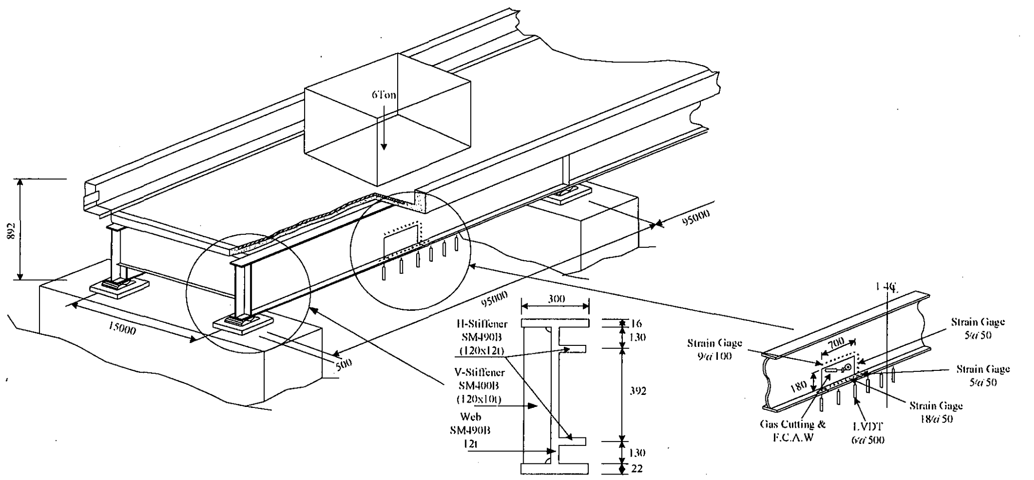


**Fig. 6 Model of repair welding experiment and dimensions.**

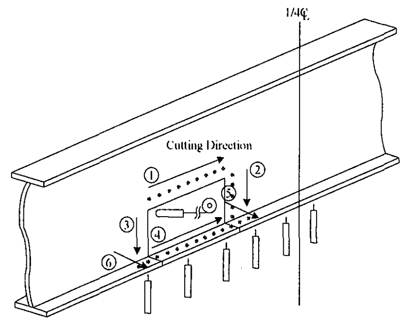


**Fig. 7 The sequence of gas cutting.**

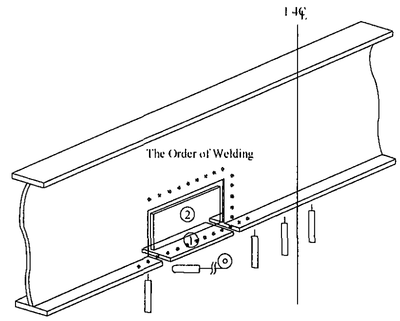


**Fig. 8 The sequence of repair welding.**

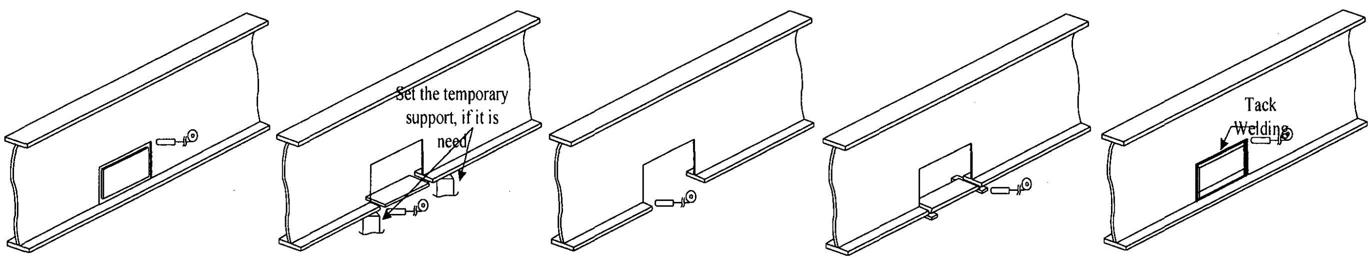


(a) Cut the web section (b) Cut the flange section (c) Make the groove (d) Weld the new web (e) Weld the new flange

**Fig. 9 Procedure of repair welding experiment.**

**Table 6 Stress of I-girder** **Units : MPa**

| Position | Allowable stress | Stress of dead load | Stress of live load | Impact coefficient |
|---|---|---|---|---|
| Lower Flange | 190 | 38 | 55 | 0.3 |

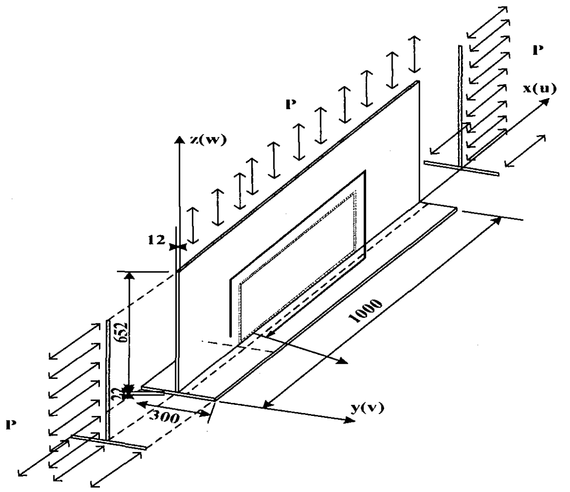


**Fig. 10 Analysis model.**

### 3.2 Condition for analysis

A 3-D full scale finite element analysis was carried out using a commercial program. The 3-D finite element analysis was performed using the idealized T-shape analysis model as in **Fig 10**. In this idealized T-shape model, the Y-Z plane and upper part of the X-Z plane are assumed to form a continuum in order to have the same conditions as a real object. The rigid displacements are restricted and the other ones are free to create the boundary conditions.

## 4. Results

### 4.1 Distortion

LVDT are set up to investigate the deflection under the lower flange and distortion due to cutting and welding. The setting position of LVDT is shown as a bar in Fig 7 and Fig 8.

*4.1.1 Distortion by cutting*

**Figure 11** shows the deflection at the cutting phase. The mark E_ represents experimental results. The other one shows the analytical results. When the cutting is performed on the web, the magnitude of the maximum deflection under the cutting surface( $x = 600mm$ ) is $1mm$ . When the cutting is carried out on the lower flange, the magnitude of the maximum deflection near to the cut surface( $x = 200, 800mm$ ) is $3.3mm$. After cutting, the distribution of residual displacement is similar to that generated while cutting. But, the magnitude of the maximum deflection is decreased. That is why thermal shrinkage occurs by cooling after heating. The rigidity of structure shows an unexpected decrease after the lower flange cutting in comparison with that after the web cutting. So, a large deflection displacement is generated under the cutting surface after the lower flange cutting. Analysis results agree with experiment results.

*4.1.2 Distortion generated by welding*

**Figure 12** shows the deflection by the welding phase. The mark E_ represents experimental results, and other one, analytical results. When welding is carried out on the lower flange, the magnitude of the maximum deflection is $0.1mm$ . After the web is welding, the magnitude of the maximum deflection unexpectedly increased. This is because the additional thermal shrinkage in the Z-direction occurred during cooling after heating in comparison with that after lower flange welding. Analysis results agree with experimental results.

### 4.2 Residual stress

Strain gauges were attached to the lower flange and web to investigate the stress generated by cutting and welding. The positions of strain gauges are shown as dots in Fig 7 and Fig 8.

**Figure 13** shows the stress component( $\sigma_x$ ) in the transverse direction for the cutting phase. The mark E_ represents experimental results, and other one, analytical results. When cutting is carried out, a compressive stress is generated on account of the thermal expansion after heating. Tensile residual stress is generated at room temperature. This is why thermal shrinkage occurs by cooling after welding. Analysis results agree with experimental results.

## 5. Conclusion

In this study, the behavior of stress and distortion generated by repair welding of steel bridges is investigated by experiment and 3-D finite element analysis. The main results can be summarized as follows.

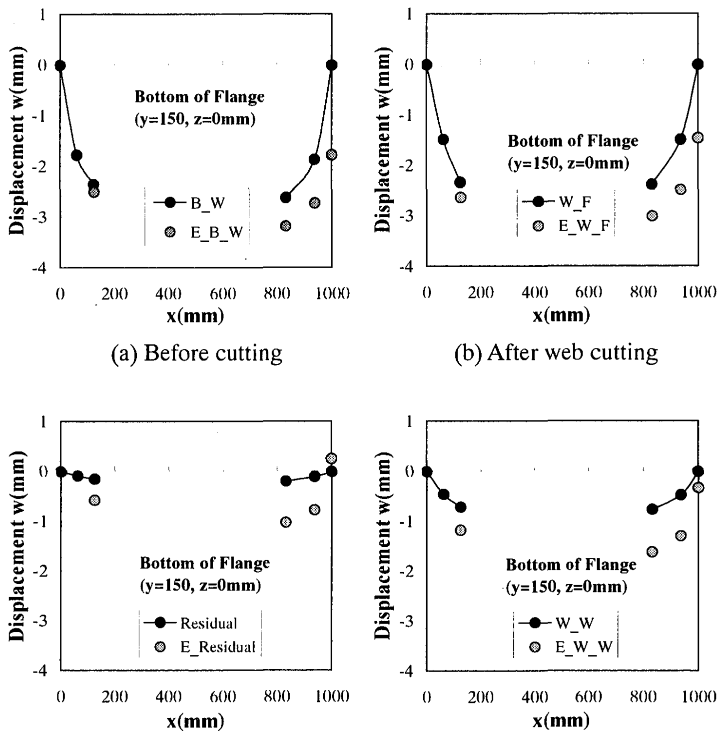


(a) Before cutting (b) After web cutting

(c) After flange cutting (d) Residual

**Fig. 11 Displacement by cutting.**

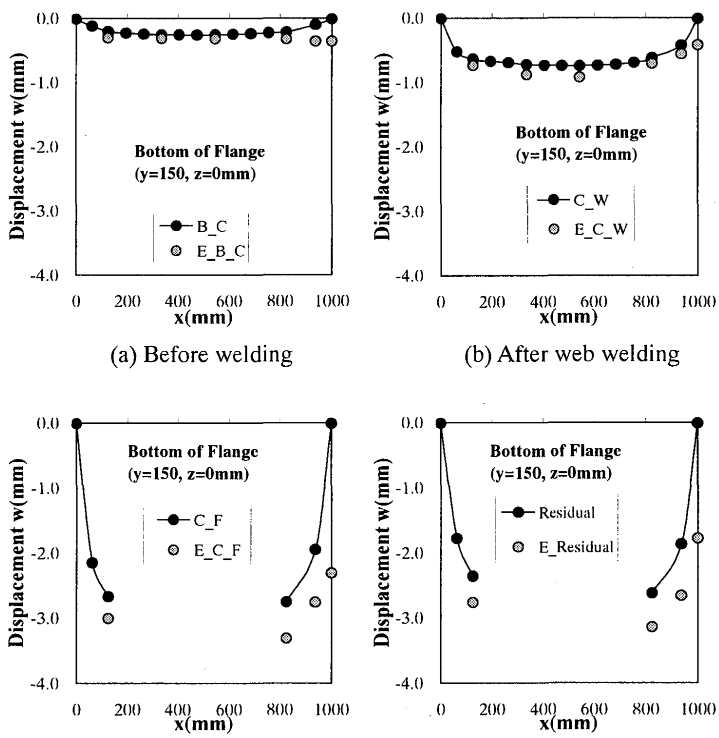


(a) Before welding (b) After web welding

(c) After flange welding (d) Residual

**Fig. 12 Displacement by welding.**

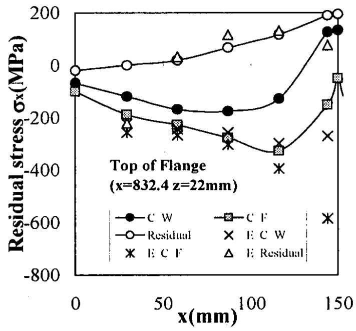


Fig. 13 Stress by cutting.

(1) The welding stress correction coefficient and the equation of load-carrying-capacity with respect to the heating were proposed in order to confirm the safety at repair work. The validity of the proposed correction coefficient and evaluation equation had been demonstrated using experimental and analytical results.

(2) When the repair work was carried out, a tensile residual stress was generated on account of shrinkage after heating.

(3) After the repair work, the residual camber displacement was increased.

## References


1) CHANG K. H., LEE S. H., JEON J. T. "Behavior of Stress and Deformation Generated by Repair Welding under Loading" KSSC, Vol. 12, No. 3, (2000), pp.269-279

2) CHANG K. H., LEE S. H., JEON J. T. "Behavior of Stress and Deformation Generated by Cutting under Loading" 6th Japan-Korea Joint Seminar on Steel Bridges, (2001), pp. 559-564

3) CHANG K. H., LEE S. H. "Characteristics of Stress and Deformation Generated by Cutting for the Repair Welding" SEWC2002, (2002), pp.431

4) CHANG K. H., LEE S. H. "Characteristics of Stress and Deformation Generated by Repair Welding under Static Loading" Proc. of KSSC, (2003), pp.51-57